

Interference of independent low-intensity light beams

L. A. Vaĭn'shteĭn(Part II), V. N. Melekhin(Parts I and II), S. A. Mishin, and E. R. Podolyak(Part I)

S. I. Vavilov Institute of Physics Problems, Academy of Sciences of the USSR, Moscow
(Submitted 21 July 1980; resubmitted 3 July 1981)
Zh. Eksp. Teor. Fiz. **81**, 2000–2012 (December 1981)

The two-photon correlation method was used to record a transient interference pattern resulting from intersection of independent laser beams. Measurements were made at low intensities in the photon counting regime at a minimum counting rate of 7×10^4 photons/sec. A quantum-electrodynamic calculation demonstrated characteristics of the interference of independent beams. The experimental results were compared with the calculations and with the earlier results of Mandel and Pfleegor [Phys. Rev. **159**, 1084 (1967); J. Opt. Soc. Am. **58**, 946 (1968)].

PACS numbers: 42.60.He, 12.20.Ds

I. EXPERIMENTS

1. Introduction

It is well known that the interference pattern formed as a result of interaction of light beams from the same source remains unchanged no matter how much its intensity is decreased, provided the recording time is sufficiently long. This underlies Dirac's theory¹ and has been confirmed experimentally on many occasions (see, for example, Refs. 2 and 3). The situation is different in the case of interference of light from independent sources. When conventional methods (for example, photographic plates or image converters) are used, it is found that the interference pattern broadens gradually and becomes indistinguishable as the light intensity is reduced. If the exposure time is short, the pattern is a set of isolated randomly distributed points at which individual photons are recorded and an increase in the exposure changes the positions of the fringes because the phase shift between the optical fields of the two beams varies randomly with time, resulting in a uniform illumination of the screen.

Interference between independent low-intensity laser beams was first recorded by employing simultaneously two photomultipliers operating in the photon-counting regime and by determining the correlation between the photocounts at points separated in space.^{4,5} We used for the same purpose a different variant of the correlation method⁶ analogous to the classical Brown-Twiss method.⁷ The use of a new method and a different optical system of the interferometer not only confirmed the occurrence of the interference, as was done by Mandel and Pfleegor earlier,^{4,5} but also enabled us to determine directly the interference pattern at much lower intensities than had hitherto been possible and to compare the results with a control interference pattern produced by one laser and recorded by the same correlation method.

Calculations given in Part II demonstrate that, in contrast to the interference of light from the same source, in the case of independent beams of sufficiently low intensities we can, in principle, determine the quantum state of the optical fields. If the beams are in a state other than coherent, then a reduction in the intensity should alter the pattern recorded by the two-

photon correlation method. This circumstance, which has been largely ignored, stresses the importance of such experiments.

2. Basic experimental layout. Selection of the apparatus parameters

We used the experimental layout shown in Fig. 1. A transient optical pattern resulting from the interference of light beams from two independent lasers is recorded with two photomultipliers operating in the photon counting regime. The voltage pulses produced by each photomultiplier, representing the emission of single photoelectrons from the photocathode, are amplified and then recorded with two counters; they are then applied simultaneously to a coincidence circuit connected to a third counter. At a constant counting rate of the n_1 and n_2 pulses in the separate channels, the coincidence counting rate n_{12} is also constant and equal to $n_{12} = 2n_1n_2\tau$, where τ is the resolution time of the coincidence circuit.

In the case under discussion the situation is different. The position of the interference pattern depends on the phase shift between the light waves and, therefore, it varies with the characteristic time $T \sim 1/\delta\omega$ governed by the difference between the laser frequencies $\delta\omega$. This frequency difference itself drifts randomly with time, mainly because of the thermal changes in the laser or resonator lengths. The probability of a photocount by each of the photomultipliers is proportional to the instantaneous intensity of light and depends on the position of the interference pattern. Therefore, the probability of photocounts by each photomultiplier varies randomly with time but the probabilities are fully correlated and the correlation is determined by the distance x between the points at which photons are detected.

The experiments give the function $\xi(x) = \bar{n}_{12}/\bar{n}_1\bar{n}_2$, where the bar represents time averaging. The calculation given in Part II shows that if $\tau \ll T$ and if classical waves of equal and constant amplitudes interfere, then $\xi(x)$ is a periodic function of x lying within the range $\tau \leq \xi(x) \leq 3\tau$ and the period L is equal to that of the instantaneous interference pattern. The average value of $\xi(x)$ equal to 2τ corresponds to random coincidences,

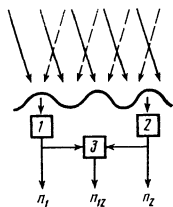


FIG. 1. Basic experimental layout: 1), 2) photomultipliers; 3) coincidence circuit.

which would be observed (for any value of x) in the case of independent modulation of light produced by each photomultiplier. It also follows from the calculations that the function $\xi(x)$ depends on the quantum state of the optical field. For any state the amplitude of the harmonic component of $\xi(x)$ is equal to τ , but the constant component does not vary on reduction in the beam intensities only in the case of a coherent state and it decreases to τ in the case of two one-photon states [see Eqs. (12) and (19) in Part II].

These results are valid only for light beams of constant amplitude, because amplitude modulation results—in the classical and quantum cases—in an increase in the average value $\xi(x)$ and can mask the quantum effect under discussion. By way of control, a transient interference pattern was formed by splitting a beam from one laser into two (as described below) and a variable phase shifter was placed on one of these beams; the pattern was then recorded by the same method involving determination of the function $\xi(x)$.

Since in the $\tau \geq T$ case the pattern became blurred and disappeared during the coincidence time and the function in question became $\xi(x) = 2\tau$, the counting circuit was switched on automatically only during those time intervals when the difference between the laser frequencies $\delta\omega$ was sufficiently small and, consequently, T was sufficiently long ($T \gg \tau$). Laser beams were split (by an optical system described below) and the frequency of beats between the independent beams was measured at a high light intensity.

In a narrow frequency range $\delta\omega$ one can assume that the laser frequencies vary with time at a certain constant rate. Consequently, the operation time of the circuit t during each run is proportional to the permissible frequency difference, i.e., to the quantity

$$\delta\omega_{\max} \sim 1/T_{\min}.$$

Since the number of counts N for each run of the measurement circuit satisfies the relationship

$$N = n_{12}t \sim n_1 n_2 t \tau,$$

it follows that N is independent of the resolution time τ , because a change in τ should be accompanied by a proportional change in T_{\min} . Bearing this point in mind, we selected sufficiently long times $\tau \approx 1 \mu\text{sec}$ and $T_{\min} \approx 5 \mu\text{sec}$, which simplified the circuit. The time interval between the moments of switching on the circuit was reduced by current windings around Invar rods fixing the distance between the mirrors in one of the lasers. A change in the current in the windings altered the length of the optical resonator (because of the magnetostriction) and this made it possible to adjust the laser frequencies.

We used LG-56 helium-neon lasers with resonators 30 cm long. The transverse modes were removed by alignment of the mirrors and the adjacent frequencies of the longitudinal modes were separated by about 500 MHz and not more than three harmonics could be emitted within a band of 1500 MHz governed by the Doppler line broadening. The triggering threshold was set so that the counting circuit was switched on only at the moments when the frequencies of the fundamental (first) harmonics of both lasers were close to the maximum of the Doppler curve and when the amplitudes of the remaining harmonics were low.

3. Optical system

The optical system is shown in Fig. 2. Light beams from two lasers 1 and 2 passed through diaphragms D_1 and D_2 with apertures 3 mm in diameter; they were then split into three components each by means of plane-parallel glass plates P_1 and P_2 . The plate thicknesses were 1.5 and 2 cm, respectively, so that the beams reflected from each plate were spatially separated by about 1 cm and had almost identical low amplitudes, whereas the main beams passed right through the plates and were then combined by mirrors M_1 and M_2 on the entry aperture of a photodiode PD. When the difference between the laser frequencies was sufficiently small, the beat signal was used to trigger the counting circuit.

The beams reflected from the plates were directed to an interferometer proposed by S.A. Mishin and consisting of the components described below. Parallel interfering beams 3 and 4, separated by a distance which could be varied, were directed by rotating a plane-parallel P_4 to a telescopic system of lenses L_1 and L_2 , whose focal points coincided. The focal lengths of the lenses were $F_1 = 35 \text{ cm}$ and $F_2 = 0.7 \text{ cm}$, respectively. After passing through the lenses the beam axes remained parallel, but the distance between them decreased by a factor of $F_1/F_2 = 50$ (Fig. 3). The beam diameters decreased by approximately the same factor and the angular divergence of the beams increased; the divergence of the original laser beams was low and amounted to 5×10^{-4} . These diverging light beams intersected and interfered as in the usual Young interferometer, except that the light sources were not formed by the slits but by focused laser beams which were brought closer together.

For the parameters of the system given above, an

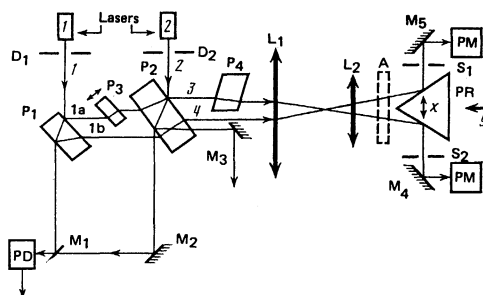


FIG. 2. Optical part of the apparatus.

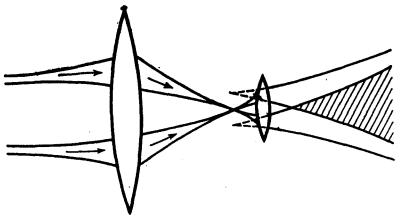


FIG. 3. Operation of the interferometer.

interference pattern of vertical fringes extending horizontally over a distance of 0.5 cm was formed already at 20 cm from the lens L_2 . The period of this pattern and, consequently, the number of fringes could be varied beginning from 2–3 right up to 10–15 by the plate P_4 which brought together or moved apart the beams. The pattern was partly absorbed by an attenuator A , which was a set of aluminized mirrors partly transmitting light and oriented at an angle to the light beam or a set of optical filters. The distance x between the points of observation was varied by a prism PR with three aluminized faces; this prism was moved in the direction y shown in Fig. 2. After reflection from the prism the light beams passed through vertical slits S_1 and S_2 ; they were then reflected by mirrors M_4 and M_5 and reached a photomultiplier PM .

The positions of the plates were selected so that the light beam $1a$ from the first laser passed through a plate 2 and coincided with the reflected beam of the second laser. In the main experiment the beam $1a$ was interrupted and the beam 3 was formed by reflecting the beam 2 so that interference between independent laser beams was observed. In control experiments, the beam 2 was interrupted and the beam $1a$ was used. In one case we obtained a steady-state interference pattern whose period and profile could be varied on any of the photomultipliers by displacing the prism or one could observe the fringes visually on a screen by removing the attenuator. In another experiment the angle of inclination of the plate P_3 was varied periodically at a frequency of tens of hertz and a transient pattern was produced which shifted at a period of 10^{-4} sec; the measurements were made using the same two-photon correlation circuit as before.

4. Electronic circuits

A block diagram of the electronic circuits is shown in Fig. 4. A beat signal from the photodiode PD passed to a V2-6 amplifier to an S1-67 oscilloscope (for direct viewing) and to an integrated circuit ST (Schmitt trigger), which produced a constant signal when the beam amplitude exceeded a certain value. Next, the signal passed through an emitter follower EF to the input of a four-channel gate circuit GC connected to four $PP-15A$ counters and the same signal was used to trigger the gate circuit. When this circuit was open, two channels counted pulses from $F\acute{E}U-79$ photomultipliers amplified in preamplifiers PA and shaped by $PD-2-1$ discriminators; the third channel passed signals from a coincidence circuit CC , whereas the fourth channel counted pulses from a $G5-54$ generator operating at a fixed frequency of 10 kHz. The number of pulses produced by

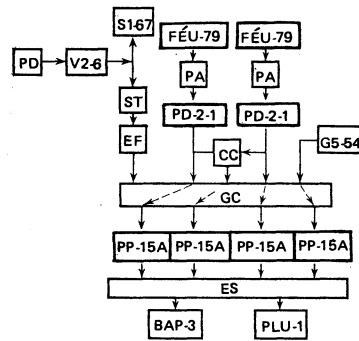


FIG. 4. Electronic circuit.

this generator was used to calibrate the time interval during which the channels were open.

The outputs of the counters were connected in turn by an electron switch ES to a $BAP-3$ printer and to a $PLU-1$ punch, which was used to record the results on punch tape; at the end of the experiment these results were analyzed (if necessary) on a computer. The gain was selected so that the circuit was triggered only by a large beat signal corresponding, as mentioned above, to practically single-frequency laser operation. The voltage applied to the photomultipliers, the gains, and the discrimination levels were selected in the course of calibration measurements in such a way as to reduce significantly the number of noise dynode pulses at the cost of just 20% loss of the useful one-electron pulses from the photocathodes.

The coincidence circuit was calibrated in a variety of ways. Weak periodic light pulses were generated by two light-emitting diodes and applied to the photomultipliers. The coincidence counting rate n_{12} was then determined as a function of the delay time between the pulses and this gave the resolution time τ . When the light-emitting diodes were operated continuously, the time τ was found from Eq. (1). The two (pulsed and continuous) methods gave the same value of the resolution time.

The intensity of the optical field in the interference pattern could be estimated knowing the quantum efficiency of the photomultiplier cathode and the attenuation of light in its path to the photocathode. These estimates were naturally not very accurate and we used the following method to determine the intensity independently. The total power of the original laser beam was measured with an $IMO-1$ power meter. Next, the beam was attenuated by multiple internal reflection in a plane-parallel optical plate. Each reflection attenuated the beam by a factor of 25, which was measured with the aid of a photodiode or a photomultiplier used in the current measuring mode; the linearity of the instruments was checked independently in the investigated range of intensities. After six reflections the beam intensity decreased by a factor of 10^8 and was finally measured in the photon counting regime by the same photomultipliers as used in the main experiments.

5. Results of measurements

A complete cycle of measurements was as follows.

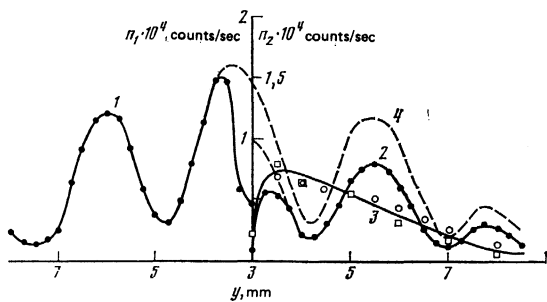


FIG. 5. Steady-state interference pattern (y is proportional to x , see Fig. 2): 1) readings of the first photomultiplier; 2) readings of the second photomultiplier; 3) envelope of interfering beams (\circ and \square); 4) results of reconstruction of curve 2.

We first aligned carefully the optical system, selected the optimal operation of the lasers, switched on the whole system and heated it for several hours. The criteria of optimal alignment and tuning were a good profile of the steady-state interference pattern and of the beat signal on the oscilloscope screen. Before a cycle of measurements and at its end the steady-state and transient interference patterns were recorded for one laser. The laser beam intensity was varied by filters and semitransparent mirrors in such a way that the photoelectron counting rate ranged from a few to tens of kilohertz. At lower intensities there were problems due to stray light (~ 500 counts/sec) and a very long time was required to obtain a number of coincidences ($\sim 10^3$) needed to ensure the required statistical accuracy. At the minimal counting rate of 2000–4000 counts/sec it was possible to increase the net counting time (i.e., the duration of observation of the beat signal) to several tens of seconds for each prism position and this was done by repeated tuning of the laser frequency. Consequently, each cycle of measurements occupied many hours and further experiments required realignment of the system.

The results of the measurements are plotted in Figs. 5–8. The steady-state (Fig. 5) and transient (Fig. 6) interference patterns from one or two lasers were recorded in the same experiment. For clarity, the counting rates in the two channels (n_1 and n_2) were plotted on different sides of the coordinate axis in Fig. 5. Although the coordinate y representing the prism position was the same for both channels, light reached different photomultipliers and was reflected from different faces of the prism (Fig. 2), so that the coordinate of the

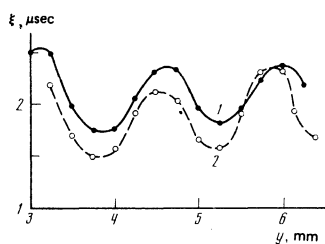


FIG. 6. Transient interference patterns: 1) interference of light from two lasers; 2) control experiment carried out using one laser.

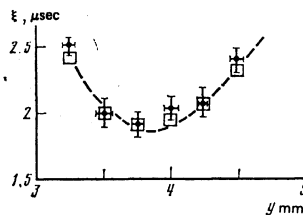


FIG. 7. Section of an interference curve obtained for different intensities of independent light beams: \square) $n \approx 17 \times 10^3$ pulses/sec; \bullet) $n \approx 3 \times 10^3$ pulses/sec.

point of observation did indeed change sign between the two channels.

The central dip in Fig. 5 was due to alignment of the prism edge with the observation plane passing through the slits S_1 and S_2 . When the interference curves were extrapolated to the observation plane (as shown by the dashed parts of the curves) and then the values in the second channel were normalized so as to match the curves in the observation plane, a complete interference pattern was obtained. Its period was fairly large (approximately 2.5 mm) and there were only three major maxima, so that it was possible to use relatively wide slits (0.2 mm) and to pass through the photomultiplier a considerable proportion of the intensity reaching the whole illuminated spot.

Figure 6 shows the transient interference pattern produced by two lasers (curve 1) and the results of a control experiment carried out using one laser (curve 2). The peak-to-peak amplitudes were similar for the two curves (± 0.25 and ± 0.3 μsec , respectively) and the slight reduction in the oscillation amplitude in the case when two lasers were used was due to the fact that it was difficult to equalize the intensities of the two laser beams, and these intensities could also vary slowly with time. This agreement between the oscillation amplitudes indicated that the contribution of the side harmonics was indeed negligible. The oscillation amplitude was considerably less than the theoretical value (± 1 μsec) and this was clearly due to the fact that the steady-state interference curve (Fig. 5) was far from ideal because the illuminated spot was reduced and the focal spots of the laser beams were relatively large so that their dimensions were comparable with the distance between the spots and this reduced the visibility. Such a complex shape of the steady-state curve prevented us from calculating accurately the shape of the transient curve expected in the experiment with one

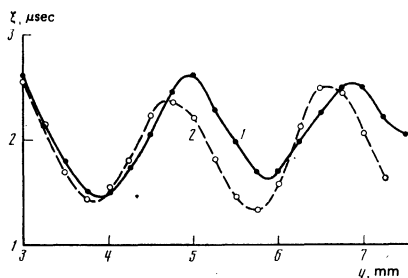


FIG. 8. Transient interference patterns: 1) two lasers; 2) one laser.

laser, and this was even more true in the case of interference of two independent beams. In particular, it was not clear why the average curve for the case of one laser was slightly below the curve representing random coincidences ($\xi = 2.1 \mu\text{sec}$) and why it rose on increase in γ .

Our control experiment on interference of beams from the same laser thus gave a pattern close to the interference pattern of independent laser beams. When the intensity was reduced, the shapes of the curves in the two cases were not affected. This was found by plotting the interference curves for two lasers in the case of intensities differing by a factor of 5–6 when the coincidence counting rate changed by a factor of about 30 (Fig. 7). At this very low intensity there were no significant changes and the result was the same as in the case of interference between independent classical waves. This was observed in all the cycles of measurements. By way of example, we plotted in Fig. 8 the transient interference curves obtained in another cycle of measurements and again the control experiment gave very similar results.

In the course of these experiments we noted an interesting fact. When a dense violet filter was used as an attenuator, the transient interference pattern produced by two lasers was not observed at all, whereas for beams from one laser the amplitude of the harmonic component was very low. When this violet filter was replaced with a set of mirrors and also when several red filters were used, interference was observed again. Special control experiments gave the following results. In addition to the emission line at 6328 \AA , the discharge tube of the laser emitted weak noncoherent radiation of different wavelengths including those in the near infrared (near the 8700 \AA line). When the attenuation was more or less uniform over the spectrum, the intensity of the noncoherent radiation was considerably less than that of the coherent radiation and it did not affect our observations. However, the violet filter 2 mm thick reduced very strongly, by about six orders of magnitude (clearly because of the resonance absorption), the 6328 \AA laser line but it hardly affected the near-infrared region ($\lambda > 7500 \text{ \AA}$). This effect predominated over the fall of the quantum efficiency of the photocathode in the $\lambda > 8300 \text{ \AA}$ range so that interference disappeared because the coherence time for the usual spectral lines was considerably less than the resolution time τ .

Calibration of the intensity by the above method and also an estimate of the light flux from the quantum efficiency of the photomultiplier indicated that the minimal counting rate in our experiments corresponded to 7×10^4 photons/sec reaching the photomultiplier photocathodes; the corresponding photon flux density was $\sim 10^6$ photons $\cdot \text{sec}^{-1} \cdot \text{cm}^{-2}$. At this density there were no special quantum features which might appear if the field of the interfering beams were in some other than coherent state (see Part II).

Mandel and Pfleeger^{4,5} used a different method for investigating interference between independent laser beams: the interference pattern was not observed di-

rectly and the light flux was 7×10^6 photons/sec. It was difficult to compare the light intensities in their and our experiments because the interferometers were of different types, but our estimates indicated that the interference beams in our experiments were approximately an order of magnitude weaker and the photon flux density was at least two orders of magnitude less than in the experiments of Mandel and Pfleeger.

II. THEORY

Quantum properties of light can, in principle, be detected by investigating the interference pattern of two independent light sources with the aid of two photodetectors. We shall now give a quantitative theory corresponding to such experiments; the results depend on the volume in which quantization occurs.

The probability of operation of an ideal photodetector (i.e., a photodetector with an instantaneous response, of point size, and with isotropic characteristics) in a time interval between t and $t + dt$ is⁸

$$w(t) dt = \eta J(\mathbf{r}, t) dt, \quad (1)$$

whereas the probability of simultaneous operation of two such detectors D and D' (at points \mathbf{r} and \mathbf{r}' after time intervals $t, t + dt$ and $t', t' + dt'$, respectively) is

$$w^{(2)}(t, t') dt dt' = \eta^2 J^{(2)}(\mathbf{r}, t; \mathbf{r}', t') dt dt', \quad (2)$$

where the constant coefficient η represents the photodetector efficiency. If the field is in a pure $\psi = |\psi\rangle$ state and it has linear polarization, then

$$J(\mathbf{r}, t) = \langle \psi | A_+(\mathbf{r}, t) A_-(\mathbf{r}, t) | \psi \rangle, \quad (3)$$

$$J^{(2)}(\mathbf{r}, t; \mathbf{r}', t') = \langle \psi | A_+(\mathbf{r}, t) A_+(\mathbf{r}', t') A_-(\mathbf{r}, t) A_-(\mathbf{r}', t') | \psi \rangle,$$

where $A = A_+ + A_-$ is the vector potential operator defined by

$$\begin{aligned} A_+(\mathbf{r}, t) &= \sum_{\lambda} a_{\lambda}^+ U_{\lambda}(\mathbf{r}, t), \\ A_-(\mathbf{r}, t) &= \sum_{\lambda} a_{\lambda} U_{\lambda}(\mathbf{r}, t), \end{aligned} \quad (4)$$

a_{λ}^+ is the photon creation operation, a_{λ} is the photon annihilation operator, and U_{λ} represents plane waves

$$U_{\lambda}(\mathbf{r}, t) = \left(\frac{2\pi\hbar c^2}{\omega_{\lambda} V} \right)^{1/2} \exp i(\mathbf{k}_{\lambda} \mathbf{r} - \omega_{\lambda} t - \phi_{\lambda}), \quad (5)$$

satisfying the condition of periodicity in a parallelepiped of volume V representing the region of intersection of light beams (V is the known as the interference volume—see Fig. 9).

Glauber⁸ defined the intensity J and the function $J^{(2)}$ by an electric field operator, but the corresponding Hamiltonian is not quite correct.⁹ If ψ corresponds to a coherent field state, then⁸

$$J^{(2)}(\mathbf{r}, t; \mathbf{r}', t') = J(\mathbf{r}, t) J(\mathbf{r}', t'); \quad (6)$$

this relationship is always satisfied in the classical theory but not in the general case.

If the field is a statistical mixture (when a state ψ_j has a probability P_j), then Eqs. (1) and (2) should be modified by replacing J and $J^{(2)}$ with \bar{J} and $\overline{J^{(2)}}$, where the averaging of the expressions in Eq. (3) is carried

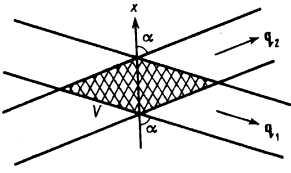


FIG. 9. Constant-phase planes of waves U_1 and U_2 in the interference region V .

out using the formula

$$\overline{\langle \Psi | A | \Psi \rangle} = \sum_j P_j \langle \Psi_j | A | \Psi_j \rangle, \quad (7)$$

and A is an arbitrary operator.

In an ideal case when each beam in the region V reduces to a plane monochromatic wave of frequency ω_l^0 , a wave vector \mathbf{k}_l^0 , and an indeterminate constant phase φ_l (see Fig. 9), the expansions in Eq. (4) contain only two waves $U_l(\mathbf{r}, t)$ and we obtain

$$\bar{J} = \bar{J}_1 + \bar{J}_2, \quad \bar{J}_l = \overline{\langle n_l \rangle} |U_l|^2 \quad (l=1, 2), \quad (8)$$

where n_l is the number of photons of frequency ω_l^0 reaching the region V from the l th beam, $\langle n_l \rangle$ is the average number of photons in a pure state, $\overline{\langle n_l \rangle}$ is the average number of photons in a mixed state; the values of \bar{J} , \bar{J}_1 , and \bar{J}_2 are constant within the region V . We then have

$$\begin{aligned} \overline{J^{(2)}(\mathbf{r}, t; \mathbf{r}', t')} &= \sum_{l, l'} \langle \langle n_l n_{l'} \rangle - \langle n_l \rangle \langle n_{l'} \rangle \rangle |U_l U_{l'}|^2 \\ &+ \sum_{l \neq l'} \langle n_l n_{l'} \rangle |U_l U_{l'}|^2 \exp i [(\omega_l^0 - \omega_{l'}^0) (t - t') - (\mathbf{k}_l^0 - \mathbf{k}_{l'}^0) (\mathbf{r} - \mathbf{r}')], \end{aligned} \quad (9)$$

where averaging is carried out only over the phases φ_l and use is made of the relationships

$$\langle n_l \rangle = \langle \psi | a_l^\dagger a_l | \psi \rangle, \quad \langle n_l n_{l'} \rangle = \langle \psi | a_l^\dagger a_l a_{l'}^\dagger a_{l'} | \psi \rangle.$$

Using the expressions in Eq. (8) and the identities

$$\langle n_l n_{l'} \rangle = \langle n_l \rangle \langle n_{l'} \rangle \quad \text{при } l \neq l', \quad \langle n_l^2 \rangle = \langle n_l \rangle^2 + \langle (\delta n_l)^2 \rangle, \quad \delta n_l = n_l - \langle n_l \rangle,$$

we can transform Eq. (9) to

$$\overline{J^{(2)}} = (\bar{J})^2 (1 + \delta^{(2)}) + 2\bar{J}_1 \bar{J}_2 \cos [(\omega_1^0 - \omega_2^0) (t - t') - (\mathbf{k}_1^0 - \mathbf{k}_2^0) (\mathbf{r} - \mathbf{r}')], \quad (10)$$

where

$$\delta^{(2)} = \frac{\langle (\delta n)^2 \rangle - \langle n \rangle^2}{\langle n \rangle^2} \quad (n = n_1 + n_2, \quad \delta n = \delta n_1 + \delta n_2) \quad (11)$$

allows for the quantum properties of the field in the interference region.

In the general case of a statistical mixture the expression (10) remains valid if in Eq. (11) we replace $\langle n \rangle$ with $\overline{\langle n \rangle}$ and also $\langle (\delta n)^2 \rangle$ with $\overline{\langle (\delta n)^2 \rangle}$; if the light beams are also randomly amplitude-modulated, the numerator includes also $\overline{(\Delta n)^2}$, which is the "classical" variance of the number of photons ($\Delta n = \langle n \rangle - \overline{\langle n \rangle}$) in the region V due to both beams.

On the right-hand side of Eq. (10) a constant term is due to the absorption of two photons from one (either) beam and the oscillatory term is due to the absorption of two photons from different beams. Quantum properties are exhibited only by the constant terms because a field giving up one photon generally gives up a second photon in a different state. In general, such a term de-

pends on the average number of photons in the region V and, consequently, on the volume of this region (for given beam intensities). In the case of a field in a coherent state we have $\delta^{(2)} = 0$, so that the quantum properties of the field are not then manifested in the interference experiments; this is due to the fact that a coherent state giving up a photon does not change so that the quantum and classical calculations give the same results for this case. When the field is in other states such that $\delta^{(2)} \neq 0$, for example, if the beams have fixed numbers of photons n_1 and n_2 , then

$$\delta^{(2)} = -\frac{1}{n_1 + n_2} = -\frac{1}{n}; \quad \delta^{(2)} = -\frac{1}{2} \quad \text{for } n_1 = n_2 = 1. \quad (12)$$

Negative values of $\delta^{(2)}$ (provided always $\delta^{(2)} > -1$) make the interference pattern clearer. This is a quantum effect which has no classical analog. It should be pointed out that in the case of interference of independent light beams the well-known Dirac hypothesis¹ that "a photon interferes only with itself" is invalid; instead of that we can formulate a different hypothesis: a photon from each beam is absorbed by one of the photodetectors D and D' but we do not know which.

Let us assume now that the wave beams are not exactly monochromatic and that their frequencies ω_l^0 drift slowly (at random and independently) and such a drift also occurs in the case of their wave vectors $\mathbf{k}_l^0 = \omega_l^0 \mathbf{q}_l / c$ (\mathbf{q}_l are constant unit vectors shown in Fig. 9). If we assume that the average values of ω_1^0 and ω_2^0 are equal to ω_0 , we can rewrite the argument of the cosine in Eq. (10) in the form

$$\begin{aligned} (\omega_1^0 - \omega_2^0) (t - t') - (\mathbf{k}_1^0 - \mathbf{k}_2^0) (\mathbf{r} - \mathbf{r}') &= \zeta_1 \tau_1 - \zeta_2 \tau_2 - \Phi, \\ \zeta_l &= \omega_l^0 - \omega_0, \quad \tau_l = t - t' - \mathbf{q}_l \frac{\mathbf{r} - \mathbf{r}'}{c} \approx t - t', \quad \Phi = \omega_0 (\mathbf{q}_1 - \mathbf{q}_2) \frac{\mathbf{r} - \mathbf{r}'}{c}. \end{aligned}$$

The coincidence circuit records photocounts separated by time intervals $|t - t'| < \tau$. The probability of double coincidences per unit time $[t = (t + t')/2]$ is

$$\begin{aligned} \overline{w^{(2)}} &= \frac{1}{2\tau} \int_{-\tau}^{\tau} \overline{w^{(2)}} \left(\bar{t} + \frac{\Phi}{2}, \bar{t} - \frac{\Phi}{2} \right) d\Phi = \eta^2 [(\bar{J})^2 (1 + \delta^{(2)}) \\ &+ 2\Lambda (\zeta_1 - \zeta_2) \bar{J}_1 \bar{J}_2 \cos \Phi], \end{aligned} \quad (13)$$

where we have ignored the difference between τ_1 and $t - t'$, and have introduced the notation

$$\Lambda(\zeta) = \frac{1}{2\tau} \int_{-\tau}^{\tau} \cos \zeta \Phi d\Phi = \frac{\sin \zeta \tau}{\zeta \tau}, \quad \zeta = \zeta_1 - \zeta_2 = \omega_1^0 - \omega_2^0. \quad (14)$$

If, moreover, the coincidence circuit is triggered only during the time interval when $|\omega_1^0 - \omega_2^0| = |\zeta| \Omega_0$, the probability of double coincidences during these intervals is

$$\overline{w^{(2)}} = \frac{1}{p_0} \int_{-a_0}^{a_0} \overline{w^{(2)}} f(\zeta) d\zeta = \eta^2 [(\bar{J})^2 (1 + \delta^{(2)}) + 2\Lambda \bar{J}_1 \bar{J}_2 \cos \Phi], \quad (15)$$

where $f(\zeta)$ is the probability density of a random quantity ζ ,

$$p_0 = \int_{-a_0}^{a_0} f(\zeta) d\zeta, \quad \Lambda = \frac{1}{p_0} \int_{-a_0}^{a_0} \Lambda(\zeta) f(\zeta) d\zeta, \quad (16)$$

and the tilde denotes averaging with respect to ζ .

We shall assume that the probability density $f(\zeta)$ satisfies the condition

$$f(\zeta) = \frac{1}{2\Omega} \quad \text{for } |\zeta| \leq \Omega.$$

and we shall also postulate that $\Omega_0 \ll \Omega_*$; then, the integrals in Eq. (16) can be calculated approximately:

$$p_0 = \frac{\Omega_0}{\Omega}, \quad \bar{\Lambda} = \frac{1}{\Omega_0 \tau} \int_0^{\Omega_0 \tau} \frac{\sin x}{x} dx, \quad (17)$$

and for $\tau = 1 \mu\text{sec}$ and $\Omega_0/2\pi = 100 \text{ kHz}$ we find that $\bar{\Lambda} \approx 0.98$. When $\Omega_0 \tau$ is increased, the quantity $\bar{\Lambda}$ decreases and the interference pattern becomes less clear.

The functions U_λ and U_l used above are, as assumed in quantum electrodynamics, plane waves of Eq. (5). In fact, we could consider other waves such as spherical (§ 7 in Ref. 10) and also waves with a complex distribution of the intensity across the beam, of the kind encountered experimentally. In the latter case, we can simply replace plane waves of Eq. (5) with wave beams

$$U_i(\mathbf{r}, t) = \left(\frac{2\pi\hbar c^2}{\omega_i} \right)^{1/2} F_i(\mathbf{r}) \exp i(\mathbf{k}_i \cdot \mathbf{r} - \omega_i t - \varphi_i), \quad (18)$$

where the complex functions $F_i(\mathbf{r})$ represent the spatial field distributions and $|F_i(\mathbf{r})|^2$ the distributions of the intensities in accordance with Eq. (8). If $\bar{J}_1/\bar{J}_2 = \text{const}$, the main relationships (10), (13), and (15) remain valid.

If the beams meet the axis x at angles α and $\pi - \alpha$ (Fig. 9), it follows from Eq. (15) that the function $\xi(x)$ introduced in Part I is given by the following expression which is valid when $\bar{J}_1 = \bar{J}_2 = \frac{1}{2}\bar{J}$ and $\bar{\Lambda} = 1$:

$$\xi(x) = 2\tau(1 + \delta^{(2)}) + \tau \cos \frac{2\pi x}{L}, \quad L = \frac{\pi c}{\omega_0 \cos \alpha} = \frac{\lambda_0}{2 \cos \alpha} \quad (19)$$

because $\bar{w}^{(2)} = \bar{n}_{12}/2\tau$ and $w = \bar{n}_1 = \bar{n}_2 = \eta\bar{J}$.

In experiments involving interference of quasimonochromatic fields an important quantity is the degeneracy parameter δ equal to the average number of photons in the coherence region or, which is equivalent, to the average number of photons passing through the coherence area during the coherence time.¹¹ If $\delta \ll 1$, interference cannot, in principle, be observed because successive photocounts or other effects of the optical field are separated by time intervals during which the interference pattern changes significantly.

However, this applies to one-photon detection methods. In the two-photon case discussed above the degeneracy parameter δ plays no role if the resolution time of the coincidence circuit is considerably less than the coherence time. In this case the quantum properties of light are governed, in accordance with Eqs. (10) and (11), by the parameter $\delta^{(2)}$ which depends on the number of photons in the normalization region V . Such a dependence on the volume of the quantization region seems initially strange, but it is an essential feature of two-photon effects at low light intensities if the field is in a state other than coherent.

It is clear from the above formulas that subject to allowance for the final width of the spectrum in the limit $V \rightarrow \infty$ we can no longer consider just one wave in each beam and instead many waves should be allowed for. Each wave has its average number of photons $\langle n_{i,\lambda} \rangle$ and variance $\langle (\delta n_{i,\lambda})^2 \rangle$; these are summed and they determine in the formula for $\delta^{(2)}$ the values of $\langle n \rangle$ and $\langle (\delta n)^2 \rangle$ which are proportional to V so that $\delta^{(2)} \rightarrow 0$ in the limit $V \rightarrow \infty$. This is to be expected because on increase in the volume V the total number of photons can become as large as we please and the quantum effects disappear.

It is therefore clear that we cannot assume that $V \rightarrow \infty$ and there is no other characteristic region except the interference one; therefore, we shall assume that V is the interference region. In our experiments the volume of this region is $V \sim 10 \text{ cm}^3$ and $\langle n \rangle \sim 10^{-3}$, so that quantum properties should appear already for $\langle n \rangle \sim 1$; therefore, we may conclude that the field of interfering beams is in a coherent state. However, there may be a very great variety of the states of a field in quantum electrodynamics and the method described above allows us to investigate such quantum states at macroscopic level although these states appear as a result of emission from individual atoms and not as a result of attenuation of coherent laser radiation. A theoretical treatment of the individual emission from atoms and its action from photodetectors has to be modified and, in particular, the question of selection of the region V need not be considered.

The authors are deeply grateful to Academician P. L. Kapitza for his interest.

- ¹P. A. M. Dirac, *The Principles of Quantum Mechanics*, 3rd ed., Clarendon Press, Oxford, 1947 (Russ. Transl., Nauka, M., 1979).
- ²J. J. Taylor, *Proc. Cambridge Philos. Soc.* **15**, 114 (1909).
- ³G. T. Reynolds, K. Spartalian, and D. B. Scarf, *Nuovo Cimento B* **61**, 355 (1969).
- ⁴R. L. Pfleeger and L. Mandel, *Phys. Rev.* **159**, 1084 (1967).
- ⁵R. L. Pfleeger and L. Mandel, *J. Opt. Soc. Am.* **58**, 946 (1968).
- ⁶V. N. Melekhin and S. A. Mishin, *Pis'ma Zh. Eksp. Teor. Fiz.* **26**, 95 (1977) [*JETP Lett.* **26**, 88 (1977)].
- ⁷R. H. Brown and R. Q. Twiss, *Proc. R. Soc. London Ser. A* **243**, 291 (1958).
- ⁸R. L. Glauber, "Optical coherence and photon statistics," in: *Quantum Optics and Quantum Radiophysics* (Russ. Transl., Mir, M., 1966, p. 91).
- ⁹L. Mandel, *Phys. Rev. A* **20**, 1590 (1979).
- ¹⁰V. B. Berestetskii, E. M. Lifshitz, and L. P. Pitaevskii, *Kvantovaya élektrodinamika* (Quantum Electrodynamics), Nauka, M., 1980, § 7.
- ¹¹J. Perina, *Coherence of Light*, Van Nostrand Reinhold, New York, 1972 (Russ. Transl., Mir, M., 1974), Chap. 2, § 3.

Translated by A. Tybulewicz